

Hopping amplitudes for Susskind fermions on random close-packed lattices (status report)

L. Polley
Institut für Physik, Oldenburg University, Germany

September 28, 2009

Abstract

Random close-pack lattices, consisting of random stacks of planar, hexagonally symmetric arrays of sites, provide a common geometric origin for $Z(3)$ symmetry and one-dimensional randomness (potentially inhibiting single-particle propagation). Due to the lack of translational symmetry in one spatial direction, there is no obvious way to determine hopping amplitudes (in fixed gauge) by analogy to Susskind fermions on a cubic spatial lattice. As is shown here, for each realisation of an rcp lattice, an infinite number of amplitude configurations exist that would be consistent with the planar $Z(3)$ and translational symmetries. By postulating stationarity of the spatial plaquette energy, which is not emerging automatically for rcp lattices, the infinity reduces to six (rather dissimilar) amplitude configurations.

Chapter 1

Introduction

Staggered lattice fermions, originally introduced as a discretisation of Dirac fermions that avoids the lattice artifact of “species doubling” to some extent [1, 2], come into focus again when spatial continuum is envisioned as approximation of a physically coarse-grained substrate. Starting out from the mathematically convenient, but stereometrically rather wasteful assumption that the substrate constitute a simple cubic lattice, and allowing a quantum particle to hop from site to neighbouring sites according to a rule constrained only by the lattice symmetries and quantum-theoretical generalities, one recovers the Susskind fermion [3, 4].

However, that neo-Maxwellian approach to relativistic propagation of matter turns out to be highly nonuniversal, being dependent on the type of lattice assumed. Close-packed lattices like face-centered cubic, or hexagonal close-packed, or random close-packed would seem to be physically well-founded choices of lattice structure. But just for the two regular of these lattices, fcc and hcp, imposing lattice symmetries modulo $U(1)$ gauge transformations on the law of propagation *rules out* relativistic propagation. Technically speaking, these lattices are just too symmetric; there is no propagation possible through first derivatives, which would be of $\mathcal{O}(a)$ with a the lattice spacing, but only “slow” propagation through second derivatives of $\mathcal{O}(a^2)$. Put differently, assuming next-neighbour hopping amplitudes of similar magnitudes on cubic and fcc/hcp lattices, coherent propagation of wavefunctions on fcc and hcp is strongly suppressed in comparison to the cubic lattice.

Hence, there is some motivation for studying random close-packed lattices, that is, random stacks of planes of honeycomb-like arrays of sites [5, 6]. The only symmetry operations are 120° rotations about axes perpendicular to the planes, and translations by one lattice spacing in six directions parallel to the planes. There is no symmetry operation relating sites on different planes. However, plaquettes are triangular, and there are two types of

Bianchi identities, tetrahedral and octahedral, by which variations perpendicular to the planes are constrained to an undetermined $Z(3)$ phase factor for each plane.

The $Z(3)$ indeterminateness shows up in the behaviour of the propagating particle under rotations by 2π , obscuring its classification as boson, fermion, or anyon. Hence, there is also motivation for imposing additional constraints on the hopping amplitudes so as to render the classification unique.

A desirable property, which on a cubic lattice would *follow* from the lattice symmetries, is that the plaquette energy (magnetic field energy, as it would be in plain $U(1)$ gauge theory) be at a local extremum. Otherwise, the configuration of hopping amplitudes would arguably be unstable. By postulating this property for hopping amplitudes on a random close-packed lattice, the indeterminateness reduces to six possible values for a global phase factor in the law of propagation.

Beyond this point, the state of affairs is rather inconclusive. A ground-state wavenumber of the particle, for the planar directions with translational symmetry, can be identified by the absence of non-countable degeneracy. For four of the parameter values, the ground-state wavefunction is localised on close-packed planes. For the two remaining parameter values, numerical study suggests that localisation still occurs at wavenumbers close to the ground-state wavenumber, but delocalisation occurs in other ranges of wavenumbers. Numerically, and so far unexplained analytically, the spectrum is found exactly symmetric under $E \rightarrow -E$ for the two parameter values, and only roughly symmetric for the other four.

In chapter 2, the basic assumptions on next-neighbour propagation with symmetries modulo gauge transformations are spelled out and exemplified by Susskind fermions on a cubic lattice. The potential modes of first-order and second-order propagation are emphasised. In chapter 3, the geometry of sites, links, and plaquettes on a general close-packed lattice is expounded. It is shown how additional symmetries of fcc and hcp lattices rule out first-order propagation. An expression for link variables in a completely fixed gauge is obtained, solely on the basis of lattice symmetries at this point. Discussion of these general links is taken up again in chapter 6, where behaviour under the symmetry rotations by 120° is made explicit, providing arguments for the anyonic nature of the particle in the general case. In chapter 4, the additional postulate of minimal plaquette energy is evaluated. In chapter 5, steps are taken towards an understanding of energy spectra and eigenfunctions.

In the approach taken here, the particle is not endowed with internal degrees of freedom. It should be noted that, on a larger scale, there could still be *apparently internal* degrees of freedom emerging from configurations of $U(1)$ gauge fields intrinsic to the lattice [1, 7, 8].

Chapter 2

Generalities, and the example of a simple cubic lattice

The basic assumption made in the following is that particle propagation from any given lattice site \vec{s} within an infinitesimal span of time is restricted to the nearest-neighbour sites $\vec{s} + \hat{n}$. Moreover, propagation is assumed to be linear and unitary, with $|\psi(\vec{s}, t)|^2$ the probability for finding the particle at site \vec{s} . Correspondingly, the wave function is assumed to satisfy an equation of the form

$$i\dot{\psi}(\vec{s}, t) = H\psi(\vec{s}, t) = \sum_{\hat{n}} l(\vec{s}, \hat{n})\psi(\vec{s} + \hat{n}, t) \quad (2.1)$$

It should be emphasised that no amplitude is included for the particle staying on-site during a step of time. There are various reasons for this. The physical interpretation of such terms is ambiguous—they may introduce a fermion mass [1], a time-component of an electromagnetic potential, or a component of a non-abelian gauge field [7, 8]. Accordingly, such terms have been treated in the literature as distortion of the most basic symmetries: breaking of chiral symmetry, or coupling of the particle to an external field. But we intend to study the propagation of a single particle free of external influences. If the particle stays on-site, it does not “probe” the locations of neighbouring sites of the lattice, so all sites should be equivalent for this channel of time evolution, and a constant on-site hopping amplitude could be absorbed in the zero point of energy. More formally, a term like $U(\vec{s})\psi(\vec{s}, t)$ would violate the translational invariances that the lattice may have, unless its dependence on x, y, z is restricted. Thus, for a first approach to propagation on random close-pack lattices, it should make sense to study the situation without an on-site amplitude.

Hermiticity of the Hamiltonian of (2.1) requires

$$l(\vec{s}, \hat{n}) = l(\vec{s} + \hat{n}, -\hat{n})^* \quad (2.2)$$

Because of equal distances to nearest neighbours, the hopping amplitudes (synonymously, link variables) are assumed to be equal in size; thus we may choose a time scale such that

$$|l(\vec{s}, \hat{n})| = 1 \quad (2.3)$$

Another key assumption is that the Hamiltonian is invariant, modulo U(1) gauge transformations, under the rotational and translational symmetry operations of the lattice, where a U(1) gauge transformation is defined by

$$\psi(\vec{s}, t) = g(\vec{s}, t)\psi'(\vec{s}, t) \quad |g(\vec{s}, t)| = 1 \quad (2.4)$$

The action of the Hamiltonian on the primed wave function is given by the gauge-transformed links

$$l'(\vec{s}, \hat{n}) = g(\vec{s} + \hat{n}, t)l(\vec{s}, \hat{n})g(\vec{s}, t)^{-1} \quad (2.5)$$

For plaquettes, which are (the smallest possible) gauge-invariant products of links, invariance modulo gauge transformations turns into strict invariance. Using the symmetry information as encoded in the plaquettes, and working in a completely fixed gauge (maximal gauge tree as in [9]), the link variables (hopping amplitudes) can be reconstructed.

2.1 Rederiving Susskind fermions on a simple cubic lattice

2.1.1 Symmetries of plaquettes

Unit vectors in the three orthogonal directions of the cubic lattice are denoted here by $\hat{1}$, $\hat{2}$, $\hat{3}$. The plaquettes (elementary closed square loop of links) are

$$p_{nm}(\vec{s}) = l_n(\vec{s})l_m(\vec{s} + \hat{n})l_n^{-1}(\vec{s} + \hat{m})l_m^{-1}(\vec{s})$$

They are assumed to be strictly invariant under all spatial translations by one unit, as well as under 90° rotations about any of the orthogonal axes of the lattice. This implies that all plaquettes are equal. Moreover, since the orientation of a plaquette is inverted by a 180° rotation, all plaquettes must equal their inverse values. This leaves only two options,

$$p_{nm}(\vec{s}) = 1 \quad \text{for all } \vec{s}, n, m \quad (\text{bosonic case}) \quad (2.6)$$

or

$$p_{nm}(\vec{s}) = -1 \quad \text{for all } \vec{s}, n, m \quad (\text{fermionic case}) \quad (2.7)$$

The classification as bosons or fermions will be justified in section 2.1.3.

2.1.2 Gauge fixing and reconstruction of links

A convenient gauge¹ for reconstructing the links and evaluating symmetries is given by

$$l_1(x, y, z) = 1 \quad l_2(0, y, z) = 1 \quad l_3(0, 0, z) = 1 \quad \text{for all } x, y, z \quad (2.8)$$

The links of direction 1 are all fixed. To reconstruct links of direction 2, one starts with such a link at position $(0, y, z)$ and proceeds in 1-direction by completing 12 plaquettes, thus obtaining a factor $(-1)^x$ in case of the fermionic plaquettes. To reconstruct links of direction 3, one starts with l_3 at position $(0, 0, z)$ and proceeds by completing 13 plaquettes in the 1-direction up to position $(x, 0, z)$, assembling a fermionic factor $(-1)^x$; from there, one proceeds by completing 23 plaquettes in the 2-direction up to position (x, y, z) , assembling another fermionic factor $(-1)^y$. In terms of the links, the two options thus are

$$l_n(\vec{s}) = 1 \quad \text{for all } \vec{s}, n \quad (\text{bosonic case}) \quad (2.9)$$

$$\begin{aligned} l_1(x, y, z) &= 1 \\ l_2(x, y, z) &= (-1)^x \\ l_3(x, y, z) &= (-1)^{x+y} \end{aligned} \quad (\text{fermionic case}) \quad (2.10)$$

The Hamiltonian of equation (2.1), with the U term omitted, takes the form

$$\begin{aligned} H\psi(x, y, z) &= \psi(x+1, y, z) + \psi(x-1, y, z) \\ &+ (-1)^x(\psi(x, y+1, z) + \psi(x, y-1, z)) \\ &+ (-1)^{x+y}(\psi(x, y, z+1) + \psi(x, y, z-1)) \end{aligned} \quad (2.11)$$

To make this resemble the Hamiltonian of a discretised Dirac equation, a change of gauge by $g(x, y, z) = i^{x+y+z}$ would be required. However, for comparison with rcp lattices, H is more conveniently presented as in (2.11).

2.1.3 Rotations by 90 degrees in the xy plane

Consider a 90° rotation, counterclockwise, about an axis parallel to the z axis, with fixed point \vec{c} . A function $\psi(x, y, z)$ is turned into

$$\psi_{90}^{\vec{c}}(x, y, z) = \psi(y + c_x - c_y, -x + c_x + c_y, z) \quad (2.12)$$

¹As to the consistency of the conditions, see [9] or [4].

When acting on links, the rotation also interchanges 1 and 2 directions². Thus the rotated links are, with simplifications due to $(-1)^2 = 1$,

$$\begin{aligned} l'_1(x, y, z) &= l_2(y + c_x - c_y, -x + c_x + c_y, z) = (-1)^{y+c_x+c_y} \\ l'_2(x, y, z) &= l_1 = 1 \\ l'_3(x, y, z) &= l_3(y + c_x - c_y, -x + c_x + c_y, z) = (-1)^{x+y} \end{aligned}$$

The same l'_1, l'_2, l'_3 are obtained, without rotation, by the gauge transformation

$$g(x, y, z) = (-1)^{xy+xc_x+xc_y+c_x^2} = g^{-1}(x, y, z) \quad (2.13)$$

Thus, expressing the symmetry modulo gauge transformations of the Hamiltonian,

$$(H\psi)_{90}^{\vec{c}}(x, y, z) = g^{-1}(x, y, z)H(g\psi_{90}^{\vec{c}})(x, y, z)$$

The c_x^2 term in the exponent of g is to ensure that a wavefunction located entirely on a fixed point of the rotation is unaffected by g as well.

The explicit form of 90° rotations can be used for an argument as to whether the spin of the wavefunction is integer or half-integer. Consider a composition of four rotations with different fixed points³, such that each site of the lattice is moving during the process but finally returning to its original position. This produces a global factor of -1 for the wavefunction in case of (2.7). In case of (2.6), all gauge factors are 1, so there can be no global change of sign. One of several possibilities is to compose rotations with fixed points at $c_x = 0, 1, 0, 1$ while $c_y = 0$. The gauge factor of the first rotation is transformed by three subsequent rotations, the factor of the second by two subsequent rotations, and so on. The collected exponents, starting with that of the last gauge transformation, are

$$(xy + x + 1) + (-xy - x + y + 1) + (xy - y + 1) + (-xy) = 3$$

2.2 Degeneracy as a ground-state criterion

Hamiltonians relating to single fermions (examples being Dirac and Susskind fermions) typically have spectra symmetric under $E \rightarrow -E$, so their ground states cannot be identified by minimal eigenvalues, but rather by minimal degeneracy.

²In the gauge used, the link variable is the same for positive and negative direction.

³The cubic lattice has an additional rotational symmetry about the axes of the dual lattice. Using these, the global change of sign is obtained by composing four equal rotations. For later comparison with rep lattices, we prefer to avoid using dual lattices.

In order for k_x^0, k_y^0, k_z^0 to be the wave numbers corresponding to a state with minimal degeneracy there should not be a continuum of other wave numbers with the same energy. Let the energy spectrum be given by the zeros of a characteristic polynomial $\chi(E, k_x, k_y, k_z)$. Let us first keep $E = E_0$ fixed. Expanding in a Taylor series about the ground-state momenta we obtain the equation

$$0 = \sum_{i=1}^3 \chi_i(k_i - k_i^0) + \frac{1}{2} \sum_{i,j=1}^3 \chi_{ij}(k_i - k_i^0)(k_j - k_j^0) + \dots$$

By a linear transformation in k -space the mixed-quadratic terms can be eliminated, so without loss of generality we may consider the simplified form

$$\begin{aligned} 0 &= \sum_{i=1}^3 \chi_i(k_i - k_i^0) + \frac{1}{2} \sum_{i=1}^3 \chi_{ii}(k_i - k_i^0)^2 + \dots \\ &= \frac{1}{2} \sum_{i=1}^3 \chi_{ii} \left(k_i - k_i^0 - \frac{\chi_i}{\chi_{ii}} \right)^2 - \sum_{i=1}^3 \frac{\chi_i^2}{\chi_{ii}} \end{aligned}$$

This is solved by infinitely many \vec{k} lying on a hyperboloid if the signs of the χ_{ii} are unequal, or an ellipsoid if the signs of the χ_{ii} are equal and some of the χ_i are nonzero. Hence, the ground-state criterion is

$$\chi_1 = \chi_2 = \chi_3 = 0 \quad \text{sign } \chi_{11} = \text{sign } \chi_{22} = \text{sign } \chi_{33} \quad \text{for finite degeneracy}$$

Now let us also consider small deviations from the ground-state energy, assuming that E_0 is an analytic, single-valued function of the wave numbers. This is the case, in particular, with hopping amplitudes depending on the direction of a link but not on the site from which the link emanates; because in such a case the Hamiltonian commutes with all translations by one unit, hence decomposes into one-dimensional sectors identified by wave numbers k_x, k_y, k_z . Thus, the leading terms in the Taylor expansion of the secular equation would be

$$0 = \chi_E(E - E_0) + \frac{1}{2} \sum_{i=1}^3 \chi_{ii}(k_i - k_i^0)(k_j - k_j^0) + \dots$$

The dispersion relation would thus not only be non-relativistic, but would also describe a ‘‘relatively static’’ propagation as discussed in section 2.3. We shall therefore assume that a ground-state must have non-zero but finite degeneracy.

2.3 Almost static options

In analogy to Susskind fermions on a cubic lattice, the symmetry arguments in the remaining chapters typically allow for a finite number of qualitatively different dispersion relations $E(k_x, k_y, k_z)$ where k_x, k_y, k_z are wavenumbers added to a constant ground-state wavenumber. In some cases (notably, fcc and hcp lattices) the dispersion relation derived is in conflict with the postulated 120° rotational symmetry, so clearly that option must be discarded. But is there a theoretical basis, as opposed to purely phenomenological, for adopting/discarding one of the options

$$E_{\text{non}} = c_{xy}(k_x^2 + k_y^2) + c_z k_z^2 \qquad E_{\text{rel}} = \sqrt{c_{xy}(k_x^2 + k_y^2) + c_z k_z^2}$$

of which the first is non-relativistic (after rescaling the z coordinate), the second relativistic? This issue will not be regarded as settled here, but it should be noted that energies of the form E_{non} and E_{rel} differ substantially in the time scales of the propagation they describe. The only dimensional parameter in the nearest-neighbour hopping amplitudes of equation (2.1), κ , equally occurs in both E_{non} and E_{rel} . Wave numbers k_x, k_y, k_z initially are dimensionless, i.e., physically measured in units of the inverse lattice spacing. Thus, for a wave function extending over a region of diameter d in physical units, the relevant dimensionless wave numbers are of order

$$k \approx \frac{1/d}{1/a}$$

Hence, the energy dispersion is proportional to the square of the lattice spacing in case of E_{non} , and is linear in the lattice spacing in case of E_{rel} . In the continuum limit $a \rightarrow 0$ this implies that E_{non} is non-propagational, or static, relative to E_{rel} . The possibility of non-relativistic propagation would need to be enforced by rescaling κ differently in both cases.

Chapter 3

Rcp links and plaquettes

3.1 Notation of link directions

A general close-pack lattice consists of hexagonal close-pack planes which are stacked in random order [5, 6]. Our general assumptions on the propagation of fermions on such lattices are, again, as listed in equations (2.1) to (2.5). To evaluate them for rcp lattices, we first need to fix a notation for the directions of links. This is done in Figure 3.1. In this notation the close-pack Bravais lattices, face-centered cubic (FCC) and hexagonal close-pack (HCP), are obtained as follows: FCC by upward directions all of the type 456 or all 789; HCP by alternating 456 and 789.

3.2 Gauge fixing

Evaluations below are greatly facilitated by working in a completely fixed gauge (maximal gauge tree as in [9]). The gauge conditions for the links are

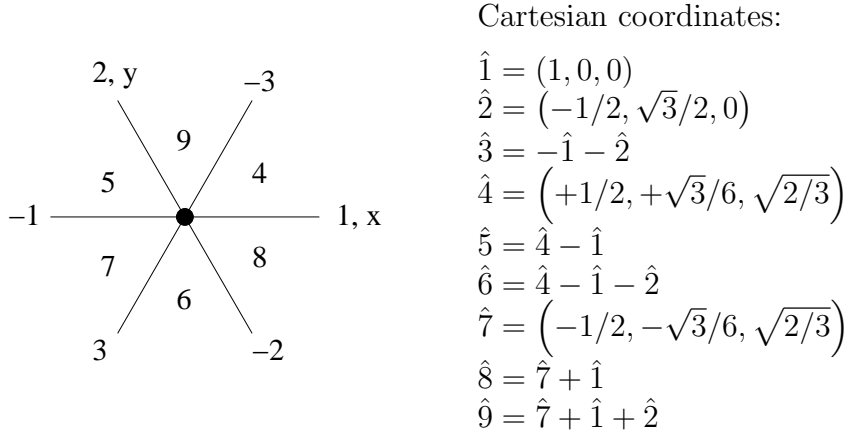
$$l_1(x, y, z) = 1 \quad l_2(0, y, z) = 1 \quad \left. \begin{array}{l} l_4(0, 0, z) \\ l_7(0, 0, z) \end{array} \right\} = 1 \quad (3.1)$$

It should be noted that these conditions are usually destroyed in a symmetry operation which is only a “symmetry modulo gauge transformation”.

3.3 Tracing the planar origin

Gauge conditions (3.1) assume that the origins $(0, 0)$ of two adjacent planes of the stack are linked by either l_4 or l_7 . In an absolute frame this implies

Figure 3.1: Definition of lattice directions. $\hat{1}, \hat{2}, \hat{3}$ lie within a close-packed plane at vertical coordinate z . $\hat{4}, \hat{5}, \hat{6}$ as well as $\hat{7}, \hat{8}, \hat{9}$ point upward (out of paper plane) to nearest neighbours in the plane $z + 1$.



that the planar origin is displaced by

$$\vec{D}(z) = d(z) \frac{\hat{4} - \hat{7}}{2} \quad z = \text{number of the plane}$$

The coefficient $d(z)$ is determined up to a constant by

$$d(z+1) = \begin{cases} d(z) + 1 & \text{in case of 456 links} \\ d(z) - 1 & \text{in case of 789 links} \end{cases} \quad (3.2)$$

For later reference we also note the following property.

$$d(z+1)^2 - d(z)^2 = \pm 2d(z) + 1 \quad \text{in case of } \begin{matrix} 456 \\ 789 \end{matrix} \quad (3.3)$$

3.4 Plaquette definitions

Plaquettes on a close-packed lattice are bordered by three links; it will be convenient to use as an index all three of the link directions involved. An overbar index is used to indicate the negative of a link direction. Under conditions (3.1), the planar plaquettes are

$$p_{123}(z) = l_2(x+1, y, z) l_3(x+1, y+1, z) \quad (3.4)$$

$$p_{132}(z) = l_3(x+1, y, z) l_2(x, y-1, z) \quad (3.5)$$

As for the interplanar plaquettes, let us first consider the 456 case. There are two types of plaquettes. Those with a base line at z and a vertex at $z+1$

are (cf. figure 3.2)

$$p_{15\bar{4}}(z) = 1 \cdot l_5(x+1, y, z) l_4^{-1}(x, y, z) \quad (3.6)$$

$$p_{26\bar{5}}(z) = l_2(x, y, z) l_6(x, y+1, z) l_5^{-1}(x, y, z) \quad (3.7)$$

$$p_{34\bar{6}}(z) = l_3(x, y, z) l_4(x-1, y-1, z) l_6^{-1}(x, y, z) \quad (3.8)$$

The plaquettes with a base line at $z+1$ and vertex at z are

$$p_{1\bar{4}5}(z+1) = 1 \cdot l_4^{-1}(x, y, z) l_5(x, y, z) \quad (3.9)$$

$$p_{2\bar{5}6}(z+1) = l_2(x-1, y-1, z+1) l_5^{-1}(x, y, z) l_6(x, y, z) \quad (3.10)$$

$$p_{3\bar{6}4}(z+1) = l_3(x, y, z+1) l_6^{-1}(x, y, z) l_4(x, y, z) \quad (3.11)$$

Secondly, we consider the case of links in the 789 directions. The plaquettes with a base line at z and vertex at $z+1$ are defined by

$$p_{17\bar{8}}(z) = 1 \cdot l_7(x+1, y, z) l_8^{-1}(x, y, z) \quad (3.12)$$

$$p_{28\bar{9}}(z) = l_2(x, y, z) l_8(x, y+1, z) l_9^{-1}(x, y, z) \quad (3.13)$$

$$p_{39\bar{7}}(z) = l_3(x, y, z) l_9(x-1, y-1, z) l_7^{-1}(x, y, z) \quad (3.14)$$

Plaquettes with a base line at $z+1$ and vertex at z are defined by

$$p_{1\bar{8}7}(z+1) = 1 \cdot l_8^{-1}(x, y, z) l_7(x, y, z) \quad (3.15)$$

$$p_{2\bar{9}8}(z+1) = l_2(x+1, y, z+1) l_9^{-1}(x, y, z) l_8(x, y, z) \quad (3.16)$$

$$p_{3\bar{7}9}(z+1) = l_3(x+1, y+1, z+1) l_7^{-1}(x, y, z) l_9(x, y, z) \quad (3.17)$$

Reverting all link directions on a plaquette, one obtains

$$p_{klm}^{-1} = p_{\bar{m}\bar{l}\bar{k}} = p_{klm}^* \quad (3.18)$$

3.5 Tetrahedral Bianchi identities

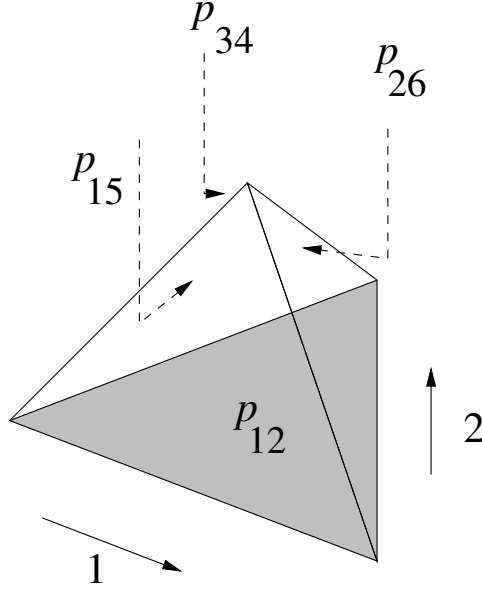
The plaquettes defined in equations (3.6), (3.7), (3.8) can be rotated into each other (rotation angle 120°) and, hence, are postulated to be equal. Moreover, the base lines of these plaquettes coincide with $p_{123}(z)$ defined in (3.4) so that there is a Bianchi identity (cf. figure 3.2)

$$p_{15\bar{4}}(z) p_{26\bar{5}}(z) p_{34\bar{6}}(z) = p_{123}(z) \quad (3.19)$$

Thus the Z_3 symmetry implies

$$p_{15\bar{4}}(z) = p_{26\bar{5}}(z) = p_{34\bar{6}}(z) = \sqrt[3]{p_{123}(z)} \quad (3.20)$$

Figure 3.2: The plaquettes in a tetrahedral Bianchi identity. By rotational symmetry, $p_{15\bar{4}}$, $p_{26\bar{5}}$, and $p_{34\bar{6}}$ are equal; this determines their relation to p_{123} up to a Z_3 phase.



Likewise, plaquettes defined in (3.9), (3.10), (3.11) can be rotated into each other and have links in common with p_{132} defined in (3.5). Therefore we have the Bianchi identity

$$p_{1\bar{4}5}(z+1)p_{2\bar{5}6}(z+1)p_{3\bar{6}4}(z+1) = p_{132}(z+1) \quad (3.21)$$

and the Z_3 symmetry implies

$$p_{1\bar{4}5}(z+1) = p_{2\bar{5}6}(z+1) = p_{3\bar{6}4}(z+1) = \sqrt[3]{p_{132}(z+1)} \quad (3.22)$$

Rotational symmetry of plaquettes (3.12), (3.13), (3.14), and the Bianchi identity due to common links with p_{13} of (3.5) imply

$$p_{17\bar{8}}(z) = p_{28\bar{9}}(z) = p_{39\bar{7}}(z) = \sqrt[3]{p_{132}(z)} \quad (3.23)$$

Rotational symmetry of plaquettes (3.15), (3.16), (3.17), and the Bianchi identity due to common links with p_{123} of (3.4) imply

$$p_{1\bar{8}7}(z+1) = p_{2\bar{9}8}(z+1) = p_{3\bar{7}9}(z+1) = \sqrt[3]{p_{123}(z+1)} \quad (3.24)$$

3.6 Failure of face-centered cubic and hexagonal close-packed lattices

These regular close-packed lattices have translational symmetries in all spatial directions. They would be considerably more practical for computer simulations than random close-pack lattices. Surprisingly, however, the discrete symmetries of these lattices fail to induce the physically desired symmetries of the propagation of single fermions in the continuum limit.

3.6.1 Fcc extra symmetries

By translational symmetry, this lattice has the same plaquette configuration on every plane. The interplanar link directions are all of the 456 variety. Moreover, there is a 180° rotational symmetry about the $\hat{1}$ axis. We note that the lattice sites may be represented by

$$\vec{s} = x\hat{1} + y\hat{2} + z\hat{4} \quad x, y, z \text{ integer} \quad (3.25)$$

The symmetry operation is (see figure 3.1)

$$\hat{1} \leftrightarrow \hat{1} \quad \hat{2} \leftrightarrow \hat{3} = -\hat{1} - \hat{2} \quad \hat{4} \leftrightarrow -\hat{5} = -\hat{4} + 1 \quad (3.26)$$

Rotating the fcc lattice site (3.25) gives another site of the same form

$$(x - y + z)\hat{1} - y\hat{2} - z\hat{4}$$

By (3.26) an interplanar plaquette $p_{15\bar{4}}$ is turned into $p_{1\bar{4}5}$, so by our basic symmetry assumption

$$p_{15\bar{4}} = p_{1\bar{4}5} =: \mu \quad (3.27)$$

Given this, all other plaquettes are determined by (3.20) and (3.22). In particular,

$$p_{123} = p_{132} = \mu^3$$

In the gauge fixed by (3.1) the corresponding links are

$$l_1 = l_2 = l_4 = 1 \quad l_5 = \mu \quad l_6 = \mu^2 \quad l_3 = \mu^3$$

as can be seen by intersertion in the definitions of section 3.4. Since the links are site-independent, the discussion of section 2.3 applies, so that propagation on a face-centered cubic lattice is “infinitely slow” in comparison to, for example, propagation on a simple cubic lattice.

Because of 3D translational symmetry of the fcc lattice, an on-site hopping term $U(\vec{s})\psi(\vec{s})$, as it was discussed and dismissed in the paragraph following equation (2.1), would reduce to $U = \text{const}$, that is, to a shift of the zero point of energy.

3.6.2 Hcp extra symmetries

For an explicit representation of the symmetry operations, let us specify the lattice by assuming that links emanating upwards from a plane with even z are of the 456 variety, while links emanating upwards from a plane with odd z are of the 789 variety. The sites of this hcp lattice can be represented as

$$\vec{s} = x\hat{1} + y\hat{2} + z\frac{\hat{4} + \hat{7}}{2} + d(z)\frac{\hat{4} - \hat{7}}{2} \quad d(z) = \begin{cases} 0 & z \text{ even} \\ 1 & z \text{ odd} \end{cases} \quad (3.28)$$

There is a 180° rotational symmetry about an axis parallel to $\hat{1} + \frac{1}{2}\hat{2}$. Its action on the link directions is (see figure 3.1)

$$\hat{1} \leftrightarrow -\hat{3} \quad \hat{2} \leftrightarrow -\hat{2} \quad \hat{4} \leftrightarrow -\hat{7} \quad (3.29)$$

This turns a site (3.28) into one of the same form with

$$x' = x \quad y' = x - y \quad z' = -z$$

The plaquette p_{123} defined by vertices $0 \rightarrow \hat{1} \rightarrow -\hat{3} \rightarrow 0$ is thus turned into its inverse $0 \rightarrow -\hat{3} \rightarrow \hat{1} \rightarrow 0$, hence $p_{123} = \pm 1$. A similar argument applies to p_{132} , so

$$p_{123} = \pm 1 \quad p_{132} = \pm 1 \quad \text{signs being independent, at } z = 0 \quad (3.30)$$

For interplanar plaquettes, by (3.30) in conjunction with (3.20), only a limited set of values is possible. Beginning with a plaquette with base line at $z = 0, \pm 2, \pm 4, \dots$ and pointing upwards,

$$p_{15\bar{4}}(z) = \mu \quad \mu^3 = \pm 1 \quad z \text{ even}$$

where invariance of plaquettes under vertical translations by two units has been used. From the latter equation we find, by applying the twofold rotation (3.29) to an axis in the plane $z = 0$ and using (3.24),

$$p_{15\bar{4}}(z) = p_{\bar{3}97}(z) = p_{3\bar{7}9}^*(z) = p_{1\bar{8}7}^*(z) \quad z \text{ even}$$

For a $p_{1\bar{4}5}$ plaquette pointing downwards from a plane at $z = \pm 1, \pm 3, \dots$ we find, by applying (3.29) to an axis in that plane and using (3.23),

$$p_{1\bar{4}5}(z) = p_{\bar{3}7\bar{9}} = p_{17\bar{8}}(z)^* \quad z \text{ odd}$$

Another symmetry of the lattice is a 180° rotation¹ about the z axis through the origin, followed by a translation by $\hat{4}$. The link directions are rotated as

$$\hat{1} \leftrightarrow -\hat{1} \quad \hat{2} \leftrightarrow -\hat{2} \quad \hat{4} \leftrightarrow \hat{7} \quad (3.31)$$

¹Equivalently, a 60° rotation

A site of the form (3.28) is turned into one of the same form with

$$x' = -x \quad y' = -y \quad z' = z + 1$$

Symmetry (3.31) relates $p_{15\bar{4}}$ to $p_{17\bar{8}}$,

$$p_{15\bar{4}}(z) = p_{\bar{1}8\bar{7}}(z + 1) = p_{17\bar{8}}^*(z + 1) \quad z \text{ even}$$

Recollecting, on the planes where they are defined (z even/odd), we have

$$p_{15\bar{4}} = p_{14\bar{5}} = \mu \quad p_{17\bar{8}} = p_{1\bar{8}7} = \mu^*$$

Give these relations, and using (3.20) and (3.22), all planar plaquettes are equal,

$$p_{123}(z) = p_{132}(z) = \mu^3 = \mu^{*3} = \pm 1 \quad \text{all } z$$

In the gauge fixed by (3.1) the corresponding links are

$$l_1 = l_2 = l_4 = l_7 = 1 \quad l_5 = l_8 = \mu \quad l_6 = l_9 = \mu^2 \quad l_3 = \mu^3$$

as can be seen by intersertion in the definitions of section 3.4. Since the links are site-independent, the discussion of section 2.3 applies, so that propagation on a hexagonal close-packed lattice is “infinitely slow” in comparison to, for example, propagation on a simple cubic lattice.

Because of symmetry (3.31) an on-site hopping term $U(\vec{s})\psi(\vec{s})$, as it was discussed and dismissed in the paragraph following equation (2.1), would reduce to $U = \text{const}$, that is, to a shift of the zero point of energy.

3.7 Reconstructing the planar links

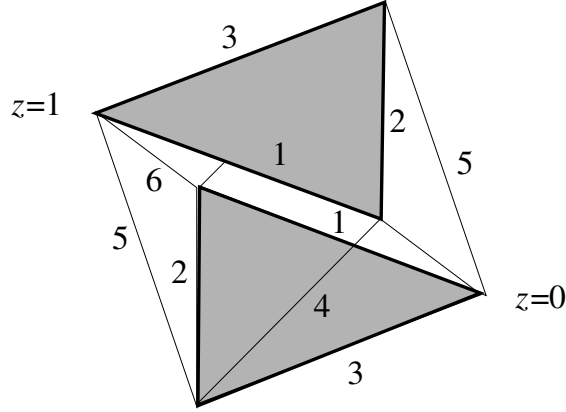
Continuing with the discussion of a general random close-packed lattice, we intend to determine the hopping amplitudes from symmetry properties of the plaquettes, so we need to solve plaquette equations for the links. This can be done recursively, starting out from the locations where the links are fixed by (3.1).

For the planar links, starting from the y axis (corresponding to the $\hat{2}$ direction) we obtain from equations (3.4) and (3.5)

$$l_2(x, y, z) = p_{12}^x(z) p_{13}^{-x}(z) \quad (3.32)$$

$$l_3(x, y, z) = p_{12}^{-x+1}(z) p_{13}^x(z) \quad (3.33)$$

Figure 3.3: An octahedral surface, relating plaquettes parallel to those of figure 3.2 to an analogous, 60° rotated set. The ensuing Bianchi identity is underlying equation (3.38).



3.8 Links in directions 456

From (3.6) and (3.9) we obtain

$$l_4(x+1, y, z) = p_{14}^{-1}(z+1)p_{15}(z)l_4(x, y, z)$$

In the gauge chosen this implies

$$l_4(x, y, z) = p_{14}^{-x}(z+1)p_{15}^x(z) \quad (3.34)$$

and by (3.9)

$$l_5(x, y, z) = p_{14}^{1-x}(z+1)p_{15}^x(z) \quad (3.35)$$

From (3.7), (3.20), (3.32), and (3.35) we finally obtain

$$l_6(x, y, z) = p_{14}^{1-x}(z+1)p_{15}^{x+1}(z)p_{12}^{-x}(z)p_{13}^x(z) \quad (3.36)$$

In these expressions for the links, $p_{15}(z)$ is assumed to be a cubic root of $p_{12}(z)$ in accord with (3.20). Using this, equations (3.6), (3.7), (3.8), and (3.9) as well as the rotational symmetry stated in (3.20) can be verified by insertion.

Inserting the links in defining equation (3.10) and exploiting the first equality of (3.22) we obtain an integrability condition. Geometrically it corresponds to the Bianchi identity depicted in figure 3.3) but it is easier to realise analytically. For all x we have

$$p_{14}(z+1) = p_{12}^{x-1}(z+1)p_{13}^{1-x}(z+1)p_{15}(z)p_{12}^{-x}(z)p_{13}^x(z)$$

Dividing the equation for $x + 1$ by that for x we obtain

$$p_{12}(z + 1) p_{13}^{-1}(z + 1) = p_{12}(z) p_{13}^{-1}(z) \quad (3.37)$$

while for $x = 0$ and using (3.37) we obtain

$$p_{14}(z + 1) = p_{12}^{-1}(z + 1) p_{13}(z + 1) p_{15}(z) \stackrel{(3.37)}{=} p_{12}^{-1}(z) p_{13}(z) p_{15}(z) \quad (3.38)$$

Raising this equation to the third power and using (3.20), (3.22) and (3.37) gives

$$p_{13}(z + 1) = \left(p_{12}^{-1}(z) p_{13}(z) \right)^2 p_{13}(z) \quad (3.39)$$

$$p_{12}(z + 1) = \left(p_{12}^{-1}(z) p_{13}(z) \right)^2 p_{12}(z) \quad (3.40)$$

Planar plaquettes at z determine planar plaquettes at $z + 1$ although, on a random close-pack lattice, there is no direct relation by a lattice symmetry. Presumably this is due to the large coordination number of 12 (compared to 6 on a cubic lattice) and to tetrahedral Bianchi identities (fig. 3.2) constraining sets of four plaquettes (instead of six).

Inserting the links in defining equation (3.11) we find that the second equality of (3.22) is automatically satisfied if we take (3.37), (3.38) and (3.39) into account. The third equality of (3.22) can be verified by using (3.38), (3.20) and (3.39).

3.9 Links in directions 789

We obtain from (3.12) and (3.15) using the gauge conditions (3.1)

$$l_7(x, z) = p_{17}^x(z) p_{18}^{-x}(z + 1) \quad (3.41)$$

and from this, using (3.15),

$$l_8(x, z) = p_{17}^x(z) p_{18}^{-x-1}(z + 1) \quad (3.42)$$

From (3.13), (3.23) and (3.32) we obtain

$$l_9(x, z) = p_{12}^x(z) p_{13}^{-x}(z) p_{17}^{x-1}(z) p_{18}^{-x-1}(z + 1) \quad (3.43)$$

Inserting the link solutions in the defining equation (3.16), and this into (3.24) using (3.32), we obtain the integrability condition

$$p_{18}(z + 1) = p_{12}^{x+1}(z + 1) p_{13}^{-x-1}(z + 1) p_{17}(z) p_{12}^{-x}(z) p_{13}^x(z)$$

Taking the quotient for $x + 1$ and x we recover equation (3.37). For $x = 0$ it here implies

$$p_{1\bar{8}}(z + 1) = p_{12}(z)p_{13}^{-1}(z)p_{17}(z) \quad (3.44)$$

Raising (3.44) to the third power and using (3.24) and (3.23) we obtain

$$p_{12}(z + 1) = \left(p_{12}(z)p_{13}^{-1}(z)\right)^3 p_{13}(z) = \left(p_{12}(z)p_{13}^{-1}(z)\right)^2 p_{12}(z) \quad (3.45)$$

3.10 Global parameters of propagation

By equation (3.37) there exists a global parameter of propagation which we define such that cubic roots, as they occur later, are uniquely specified:

$$p_{12}(z)^{-1} p_{13}(z) = \text{const} =: \lambda^3 \quad (3.46)$$

Thus, in each z plane we have

$$p_{13}(z) = \lambda^3 p_{12}(z) \quad (3.47)$$

The relation between planar plaquettes at z and $z + 1$, using (3.40) or (3.45), respectively, is

$$456 : \quad p_{12}(z + 1) = p_{12}(z)\lambda^6 \quad (3.48)$$

$$789 : \quad p_{12}(z + 1) = p_{12}(z)\lambda^{-6} \quad (3.49)$$

These relations can be integrated using the origin-displacement function $d(z)$ defined in section 3.3. Selecting a cubic root of $p_{12}(0)$ by writing

$$p_{12}(0) = \mu^3$$

we obtain from (3.48) and (3.49)

$$p_{12}(z) = \lambda^{6d(z)} \mu^3 \quad (3.50)$$

For the interplanar plaquettes, (3.38) and (3.20), or (3.44) and (3.24), respectively, imply

$$\begin{aligned} p_{1\bar{4}}(z + 1) &= \lambda^3 p_{15}(z) = \lambda^{2d(z)+3} \mu \zeta_z \\ p_{17}(z) &= \lambda^3 p_{1\bar{8}}(z + 1) = \lambda^{2d(z)+1} \mu \zeta_z^{-1} \end{aligned} \quad \text{where } \zeta_z \in \{1, e^{2\pi i/3}, e^{-2\pi i/3}\} \quad (3.51)$$

Analogous relations for the remaining (120° rotated) plaquettes can be obtained immediately from (3.20) and (3.24). Solving for the links by using (3.32) to (3.36), (3.41) to (3.43), and (3.51), we obtain

$$\begin{aligned}
l_1 &= 1 \\
l_2 &= \lambda^{-3x} \\
l_3 &= \lambda^{3x+6d(z)} \mu^3 \\
l_4 &= \lambda^{-3x} \\
l_5 &= \lambda^{3-3x+2d(z)} \mu \zeta_z \\
l_6 &= \lambda^{4d(z)+3} \mu^2 \zeta_z^2 \\
l_7 &= \lambda^{3x} \\
l_8 &= \lambda^{2+3x-2d(z)} \mu^{-1} \zeta_z \\
l_9 &= \lambda^{1-4d(z)} \mu^{-2} \zeta_z^2
\end{aligned} \tag{3.52}$$

This appears to be as far as one can get in reducing the possible configurations of hopping amplitudes by symmetry considerations alone. There are two global parameters, λ and μ , of modulus 1 but otherwise unrestricted, and for each plane there is an undetermined Z_3 phase factor, ζ_z . Any link configuration of the form (3.52) has planar translational and 120° rotational symmetry, both modulo gauge transformations, details of which are given in chapter 6. The behaviour under three composed 120° rotations, discussed in section 6.3, suggests that λ is some sort of a spin parameter, since a global phase factor of $\lambda^{-1} \bmod Z_3$ is generated by the 360° rotation. Integer spin would correspond to $\lambda \in Z_3$, half-integer spin to $-\lambda \in Z_3$. For other values of λ , the argument would suggest that hopping amplitudes (3.52) describe anyons. The latter possibility is removed by postulating, in addition to the symmetries of plaquettes, that the plaquette energy be minimal. If we further restrict ourselves to fermions, configuration (3.52) will be shown to reduce to (4.16).

Chapter 4

Minimising the plaquette energy

In U(1) lattice gauge theory, the dynamics of the gauge field is derived from an action which is the sum of all real parts of plaquettes. In particular, the magnetic field energy is given by the real parts of all spatial plaquettes. For this energy to be in a minimum, the action must be stationary under infinitesimal changes of each link variable. In the case of a simple cubic lattice, the stationary point of

$$\sum_{ij} \operatorname{Re}(p_{ij}) = \sum_{ij} \cos(\arg p_{ij}) \quad (4.1)$$

is automatically attained for free Susskind fermions; all spatial plaquettes are equal to -1 in this case. On a random-stack lattice, however, stability of the plaquette action poses an additional constraint on parameters λ, μ, ζ_z of equations (3.52), compensating for the lack of symmetry the z direction.

4.1 Variations of planar plaquettes

By the assumed symmetry under 120° rotations, the sum of cosines of plaquettes containing one of the interplanar links, l_4, \dots, l_9 , is automatically stable under infinitesimal variations of that link. Constraints on the values of λ and μ may only result from postulating stability under variations of planar links, of which it suffices to consider l_1 . In a plane z which has links of the variety 456 both above and below it, l_1 occurs in plaquettes $p_{12}(z) \equiv p_{123}(z)$, $p_{13}(z) \equiv p_{132}(z)$, $p_{15}(z) \equiv p_{15\bar{4}}(z)$, and $p_{1\bar{4}}(z) \equiv p_{1\bar{4}5}(z)$, where in the equivalent notations all links contained in a plaquette are listed explicitly. Stationarity requires that the derivative of (4.1) with respect to

any particular l_1 vanish. Collecting the links as given by (3.52) and using $d(z-1) = d(z) - 1$, the condition for stationarity at a 456/456 junction is

$$\begin{aligned}
& \sin(6d(z) \arg \lambda + 3 \arg \mu) \\
+ & \sin((6d(z) + 3) \arg \lambda + 3 \arg \mu) \\
+ & \sin(2d(z) \arg \lambda + \arg \mu + \arg \zeta_z) \\
+ & \sin((2d(z) + 1) \arg \lambda + \arg \mu + \arg \zeta_{z-1}) = 0
\end{aligned} \tag{4.2}$$

In a plane z which has links of the variety 789 both above and below it, links l_1 occur in the plaquettes $p_{12}(z) \equiv p_{123}(z)$, $p_{13}(z) \equiv p_{132}(z)$, $p_{17}(z) \equiv p_{178}(z)$, and $p_{18}(z) \equiv p_{187}(z)$. Stationarity at a 789/789 junction thus requires

$$\begin{aligned}
& \sin(6d(z) \arg \lambda + 3 \arg \mu) \\
+ & \sin((6d(z) + 3) \arg \lambda + 3 \arg \mu) \\
+ & \sin((2d(z) + 1) \arg \lambda + \arg \mu - \arg \zeta_z) \\
+ & \sin(2d(z) \arg \lambda + \arg \mu - \arg \zeta_{z-1}) = 0
\end{aligned} \tag{4.3}$$

In a plane z which has links of the variety 456 below it and of the variety 789 above it, links l_1 occur in the plaquettes $p_{12}(z) \equiv p_{123}(z)$, $p_{13}(z) \equiv p_{132}(z)$, $p_{17}(z) \equiv p_{178}(z)$, and $p_{14}(z) \equiv p_{145}(z)$. Stationarity under variations of l_1 at a 456/789 junction thus requires

$$\begin{aligned}
& \sin(6d(z) \arg \lambda + 3 \arg \mu) \\
+ & \sin((6d(z) + 3) \arg \lambda + 3 \arg \mu) \\
+ & \sin((2d(z) + 1) \arg \lambda + \arg \mu - \arg \zeta_z) \\
+ & \sin((2d(z) + 1) \arg \lambda + \arg \mu + \arg \zeta_{z-1}) = 0
\end{aligned} \tag{4.4}$$

If the 789 layer is below and 456 above the z plane, instead of $p_{178}(z)$ and $p_{145}(z)$ we have the plaquettes $p_{187}(z)$ and $p_{154}(z)$. Stationarity under variations of l_1 at a 789/456 junction thus requires

$$\begin{aligned}
& \sin(6d(z) \arg \lambda + 3 \arg \mu) \\
+ & \sin((6d(z) + 3) \arg \lambda + 3 \arg \mu) \\
+ & \sin(2d(z) \arg \lambda + \arg \mu + \arg \zeta_z) \\
+ & \sin(2d(z) \arg \lambda + \arg \mu - \arg \zeta_{z-1}) = 0
\end{aligned} \tag{4.5}$$

Equations (4.2) to (4.5) must hold for any integer $d(z)$ since, on an infinite random stack, a sequence of 456/456 and 456/789 interplanar links will occur somewhere in conjunction with any horizontal displacement of the planar origin. Parameters λ and μ are the same in all equations, while the $\zeta \in \mathbb{Z}_3$ are not otherwise determined, so for each d the equation at the respective junction need only hold for one of the possible combinations of ζ_z and ζ_{z-1} .

4.2 Links constant in x

A special situation occurs if $\lambda^3 = 1$ so that, under the sines in equations (4.2) to (4.5), the $\arg \lambda$ terms can be absorbed in the Z_3 phases. All four equations thus take the form (using Euler's formula)

$$2\mu^3 - 2\mu^{-3} + (\zeta_1 + \zeta_2)\mu - (\zeta_1^{-1} + \zeta_2^{-1})\mu^{-1} = 0 \quad \zeta_{1,2} \in Z_3$$

with the solutions

$$\mu = \begin{cases} \zeta_1^{-1}, i\zeta_1^{-1}, -\zeta_1^{-1}, -i\zeta_1^{-1} & \text{for } \zeta_2 = \zeta_1 \\ \pm\zeta_1\zeta_2, (\pm\frac{1}{4}\sqrt{6} + \frac{1}{4}i\sqrt{10})\zeta_1\zeta_2, (\pm\frac{1}{4}\sqrt{6} - \frac{1}{4}i\sqrt{10})\zeta_1\zeta_2 & \text{for } \zeta_2 \neq \zeta_1 \end{cases}$$

This amounts to 24 different values that μ can take. For each of them, on any random close-pack lattice, we find by inserting in the appropriate sequence of equations (4.2) to (4.5) that a unique sequence of ζ_z exists such the stability conditions are satisfied.

In the present case, the links (3.52) become independent of x . This probably means we are dealing with a system with zero spin, and we will not consider it any further here.

4.3 Links alternating in x

In equations (4.4) and (4.5) there are only six combinations of ζ_z and ζ_{z-1} to consider: three with equal values of $\arg \zeta_z$ and $-\arg \zeta_{z-1}$, and three with different values. In the latter case,

$$\sin(\alpha + \arg \zeta_1) + \sin(\alpha + \arg \zeta_2) = -\sin(\alpha + \arg \zeta_3) \quad \zeta_1 \neq \zeta_2$$

where ζ_3 is the missing element of Z_3 . When taking the product over those six combinations, we encounter expressions of the form

$$\begin{aligned} & [A + B \sin \alpha] [A + B \sin(\alpha + 2\pi/3)] [A + B \sin(\alpha - 2\pi/3)] \\ & = A^3 - \frac{3}{4}AB^2 - \frac{1}{4}B^3 \sin 3\alpha \end{aligned} \quad (4.6)$$

where $B = 2$ in the cases of equal ζ and $B = -1$ in the cases of unequal ζ . Moreover, we have $A = x + y$ with

$$\begin{aligned} x &= \sin(6d(z) \arg \lambda + 3 \arg \mu) \\ y &= \sin((6d(z) + 3) \arg \lambda + 3 \arg \mu) \end{aligned} \quad (4.7)$$

In the product over the six cases of (4.4), using (4.6) we find $\sin 3\alpha = y$, so that

$$\left[(x+y)^3 - 5y - 3x\right] \left[(x+y)^3 - \frac{1}{2}y - \frac{3}{4}x\right] = 0 \quad (4.8)$$

In the product over the six cases of (4.5) we find $\sin 3\alpha = x$. This gives the previous equation with x and y interchanged,

$$\left[(x+y)^3 - 5x - 3y\right] \left[(x+y)^3 - \frac{1}{2}x - \frac{3}{4}y\right] = 0 \quad (4.9)$$

If we had $x \neq y$ the equations would imply

$$(x+y)^3 - 5y - 3x = 0 \quad (x+y)^3 - \frac{1}{2}x - \frac{3}{4}y = 0$$

or the same with x and y interchanged. The solutions (up to interchange) would be $x = \pm\sqrt{\frac{10100}{19683}}$ and $y = \frac{17}{10}x$. This is ruled out by $|x| \leq 1$ and $|y| \leq 1$. So we must have

$$x = y$$

Both (4.8) and (4.9) are then solved by

$$x = y = 0, \pm 1, \pm\sqrt{\frac{5}{32}} \quad (4.10)$$

Inserting this into (4.7) at $d = 0$ we obtain the possible values for the parameters μ and λ . One possibility is $3 \arg \lambda = 2\pi n$, the case discussed and discarded in section 4.2. The other possibility is that λ and μ are related by

$$\arg \lambda = (2n+1)\frac{\pi}{3} - 2 \arg \mu \quad n \text{ integer} \quad (4.11)$$

Assuming this, it turns out that $x = y = \pm\sqrt{5/32}$ correspond to λ and μ that do *not* solve (4.8) and (4.9) at $d = 1$. In contrast, for $x = y = 0, \pm 1$ we find $\arg \mu$ restricted to a multiple of $\pi/6$, so that x and y in (4.7) become independent of d . For μ an odd multiple of $\pi/6$, λ is in the class of section 4.2 again. The only options of interest (non-zero spin) therefore are

$$\arg \lambda = (2n+1)\frac{\pi}{3} \quad \arg \mu = m\frac{\pi}{3} \quad n, m \text{ integer} \quad (4.12)$$

Thus the links (3.52) become dependent on x through a factor $(-1)^x$. In each of equations (4.2) to (4.5), the first two sines cancel. In (4.2) the remaining terms can be rewritten, using $d(z) = d(z-1) + 1$, as

$$\sin(2d(z) \arg \lambda + \arg \mu + \arg \zeta_z) + \sin((2d(z-1)+3) \arg \lambda + \arg \mu + \arg \zeta_{z-1}) = 0$$

Since $3 \arg \lambda$ here is an odd multiple of π , the last equation implies that the sines of the arguments of l_5 must be equal on two subsequent planes. For angles which are either all even or all odd multiples of $\pi/3$ (depending on whether $\arg \mu$ is an even or odd multiple) equality of sines implies equality of the angles modulo 2π , hence

$$l_5(x, z) = l_5(x, z - 1) \quad (4.13)$$

Analogously, the remaining terms in (4.4) can be rewritten, extracting a phase shift of π at $z - 1$ and using $\sin \alpha = \sin(\pi - \alpha)$ at z , as

$$\sin((2 - 2d(z)) \arg \lambda - \arg \mu + \arg \zeta_z) = \sin(2d(z - 1) \arg \lambda + \arg \mu + \arg \zeta_{z-1})$$

Again, this is a case where equality of sines implies equality of the arguments. Comparing with (3.52) we thus find

$$l_8(x, z) = -l_5(x, z - 1) \quad (4.14)$$

Equation (4.5) shows that the same must hold with the roles of z and $z - 1$ interchanged, hence

$$l_5(x, z) = -l_8(x, z - 1) \quad (4.15)$$

Equations (4.13), (4.14) and (4.15) imply that a link l_5 is the same wherever it occurs; likewise for l_8 and for the squared links l_6 and l_9 . Hence, assuming (4.12) for stability of the plaquette action, link expressions (3.52) reduce to

$$\begin{aligned} l_1 &= 1 \\ l_2 &= (-1)^x \\ l_3 &= \eta^3 (-1)^x \\ l_4 &= (-1)^x \\ l_5 &= -\eta (-1)^x & \eta^6 &= 1 \\ l_6 &= -\eta^2 \\ l_7 &= (-1)^x \\ l_8 &= \eta (-1)^x \\ l_9 &= -\eta^2 \end{aligned} \quad (4.16)$$

where η can be identified, for example, as

$$\eta = \mu \zeta_{z_0} \quad \text{at some } l_5 \text{ with } d(z_0) = 0$$

Since l_5 and l_8 no longer depend on z , the Z_3 phase factors and the horizontal shifts $d(z)$ in expressions (3.52) are correlated by

$$\zeta_z = \eta \mu^{-1} \lambda^{-2d(z)} \text{ for links } l_5, l_6 \quad \zeta_z = \eta \mu \lambda^{2d(z)-2} \text{ for links } l_8, l_9$$

Moreover, interplanar plaquettes like (3.6) and (3.12) become constants,

$$p_{15\bar{4}} = \eta \quad p_{17\bar{8}} = -\bar{\eta}$$

Chapter 5

Towards energy eigenfunctions

For solutions to the equation of propagation (2.1) the expressions (4.16) imply that we only need to consider superpositions of two basis functions of the form

$$\psi_1(\vec{s}, t) = e^{ik_x x} e^{ik_y y} f(z) \quad \text{and} \quad \psi_2(\vec{s}, t) = (-1)^x e^{ik_x x} e^{ik_y y} g(z). \quad (5.1)$$

Thus, an energy eigenfunction must satisfy the recurrence relation

$$E\Psi_z = H_{\text{up}}\Psi_{z+1} + H_{\text{planar}}\Psi_z + H_{\text{down}}\Psi_{z-1} \quad (5.2)$$

where H_{up} , H_{planar} , H_{down} are 2×2 matrices, and

$$\Psi_z = \begin{pmatrix} f(z) \\ g(z) \end{pmatrix} \quad (5.3)$$

5.1 Construction of hopping matrices

By (4.16) a site (x, y, z) “receives” its contribution from the neighbouring sites of the plane with amplitudes as follows. (using hermiticity (2.2))

$$\begin{array}{ll} (x \pm 1, y, z) & 1 \\ (x, y \pm 1, z) & (-1)^x \\ (x \mp 1, y \mp 1, z) & \pm(-1)^x \eta^{\pm 3} \end{array} \quad (5.4)$$

In case of a 456 position of the upper plane, the corresponding hopping amplitudes are

$$\begin{array}{ll} (x, y, z + 1) & (-1)^x \\ (x - 1, y, z + 1) & -(-1)^x \eta \\ (x - 1, y - 1, z + 1) & -\eta^2 \end{array} \quad (5.5)$$

Hopping amplitudes connecting to the lower plane, in case of an inverse 456 position ¹ are obtained by hermiticity (2.2)) from (5.5)

$$\begin{array}{ll} (x, y, z - 1) & (-1)^x \\ (x + 1, y, z - 1) & (-1)^x \eta^{-1} \\ (x + 1, y + 1, z - 1) & -\eta^{-2} \end{array} \quad (5.6)$$

In case of a 789 position of the upper plane, we have instead

$$\begin{array}{ll} (x, y, z + 1) & (-1)^x \\ (x + 1, y, z + 1) & (-1)^x \eta \\ (x + 1, y + 1, z + 1) & -\eta^2 \end{array} \quad (5.7)$$

while for an inverse 789 position we have from (5.7) by hermiticity

$$\begin{array}{ll} (x, y, z - 1) & (-1)^x \\ (x - 1, y, z - 1) & -(-1)^x \eta^{-1} \\ (x - 1, y - 1, z - 1) & -\eta^{-2} \end{array} \quad (5.8)$$

From these we can find the hopping matrices of equation (5.2), applying the general rule that columns contain the images of canonical basis vectors, here corresponding to the basis functions (5.1). Thus,

$$H_{\text{up}}^{456} = \begin{pmatrix} -\eta^2 e^{-ik_x} e^{-ik_y} & 1 + \eta e^{-ik_x} \\ 1 - \eta e^{-ik_x} & \eta^2 e^{-ik_x} e^{-ik_y} \end{pmatrix} \quad H_{\text{down}}^{456} = (H_{\text{up}}^{456})^\dagger \quad (5.9)$$

$$H_{\text{up}}^{789} = \begin{pmatrix} -\eta^2 e^{ik_x} e^{ik_y} & 1 - \eta e^{ik_x} \\ 1 + \eta e^{ik_x} & \eta^2 e^{ik_x} e^{ik_y} \end{pmatrix} \quad H_{\text{down}}^{789} = (H_{\text{up}}^{789})^\dagger \quad (5.10)$$

$$\begin{aligned} H_{\text{planar}} & \quad (5.11) \\ & = 2 \begin{pmatrix} \cos k_x & \cos k_y + i \sin(k_x + k_y - 3 \arg \eta) \\ \cos k_y - i \sin(k_x + k_y - 3 \arg \eta) & -\cos k_x \end{pmatrix} \end{aligned}$$

5.2 Points of transparency

Well-known results on Anderson's model and variants [10] suggest that 1-dimensionally random conditions of propagation cause localisation of energy eigenfunctions. Hence, propagation on rcp lattices in the z direction should be inhibited for almost all wavenumbers k_x, k_y . However, at isolated points in k space,

$$e^{ik_x} = \pm i \quad \text{and independently} \quad e^{ik_y} = \pm i$$

¹That is, the plane z is in a 456 position relative to the plane $z - 1$

the randomness disappears since propagation through 456 and 789 links becomes indistinguishable. In fact, at these points

$$H_{\text{up}}^{456} = H_{\text{up}}^{789} =: H_{\text{up}} \quad H_{\text{planar}} = 0$$

There are two cases to consider.

5.2.1 Eta real

For $\eta = \pm 1$ the hopping matrices are selfadjoint, so

$$H_{\text{up}} = H_{\text{down}}$$

Let us concentrate on $\eta = 1$ and planar momenta $e^{ik_x} = e^{ik_y} = i$, since for other choices of signs the conclusions are analogous. Expanding energy eigenfunctions in an eigenbasis of the matrix,

$$\Psi(z) = \alpha_z \begin{pmatrix} 1 - i \\ \sqrt{3} - 1 \end{pmatrix} + \beta_z \begin{pmatrix} i - 1 \\ \sqrt{3} + 1 \end{pmatrix}$$

and inserting eigenvalues $\pm\sqrt{3}$, we find that equation (5.2) translates into

$$\begin{aligned} \sqrt{3}\alpha_{z+1} + \sqrt{3}\alpha_{z-1} &= E\alpha_z \\ -\sqrt{3}\beta_{z+1} - \sqrt{3}\beta_{z-1} &= E\beta_z \end{aligned}$$

The non-diverging solutions are

$$\left. \begin{aligned} \alpha_z &= \alpha_0 e^{i\gamma z} \\ \beta_z &= \beta_0 (-1)^z e^{i\gamma z} \end{aligned} \right\} \quad \text{where} \quad E = 2\sqrt{3} \cos \gamma$$

In order to obtain information for k_x and k_y slightly different from $\pi/2$, recursion (5.2) can be integrated numerically on a one-dimensional lattice in the z direction. According to [11] the difference between energy eigenvalues obtained with periodic and antiperiodic boundary conditions can be used as a criterion for the localisation properties of the wave function; see Figure 5.1.

Spectrum is symmetric—unexplained

Figures 5.1 are symmetric under $E \rightarrow -E$. So far, this is just a numerical finding. It depends on the realness of η , and the symmetry operation appears to be nonlocal in z , and not simply related to a reflection $z \rightarrow -z$. Transformations of the plaquette and link configuration that might be relevant for an analytical understanding are listed below; this collection does not suffice, however, to equate any the transformed configurations to the original one.

- Hamiltonian is invariant under complex conjugation.
- Spectrum is the same in sectors determined by wavenumbers (k_x, k_y) and by $(-k_x, -k_y)$ (using complex conjugation).
- Spectrum is the same on a lattice with 456 and 789 links interchanged and η replaced by $-\eta$, since this is the original configuration rotated by 180° about an axis perpendicular to the planes.
- $\eta \rightarrow -\eta$ implies $E \rightarrow -E$ since both are generated by unitary transformation with Pauli matrix σ_2 at each z .
- Spectrum is inverted ($E \rightarrow -E$) if the sequence of 456 and 789 links is inverted ($z \rightarrow -z$); this follows by combining the two previous operations with the 180° rotation (3.29).

It should be noted that there is no 2×2 matrix anticommuting with all three matrices in equations (5.9), (5.10), (5.11) since these are three linearly independent combinations of the Pauli matrices.

5.2.2 Eta non-real

For $\eta = e^{\pm\pi i/3}$ and $\eta = -e^{\pm\pi i/3}$ the hopping matrices are defective. Let us concentrate on the planar momenta $e^{ik_x} = e^{ik_y} = i$. We then find, using $1 + \eta^2 + \eta^{*2} = 0$, the dyadic representation

$$H_{\text{up}} = \begin{pmatrix} \eta & \\ \eta^* + i & \end{pmatrix} \begin{pmatrix} \eta & \eta^* - i \\ & \end{pmatrix}$$

$$H_{\text{down}} = \begin{pmatrix} \eta^* & \\ \eta + i & \end{pmatrix} \begin{pmatrix} \eta^* & \eta - i \\ & \end{pmatrix}$$

Expanding the energy eigenfunction in the basis of the two column vectors,

$$\Psi(z) = \alpha_z \begin{pmatrix} \eta \\ \eta^* + i \end{pmatrix} + \beta_z \begin{pmatrix} \eta^* \\ \eta + i \end{pmatrix}$$

equation (5.2) translates into

$$(3 + 2 \sin \arg \eta) \beta_{z+1} = E \alpha_z \quad (3 - 2 \sin \arg \eta) \alpha_{z-1} = E \beta_z$$

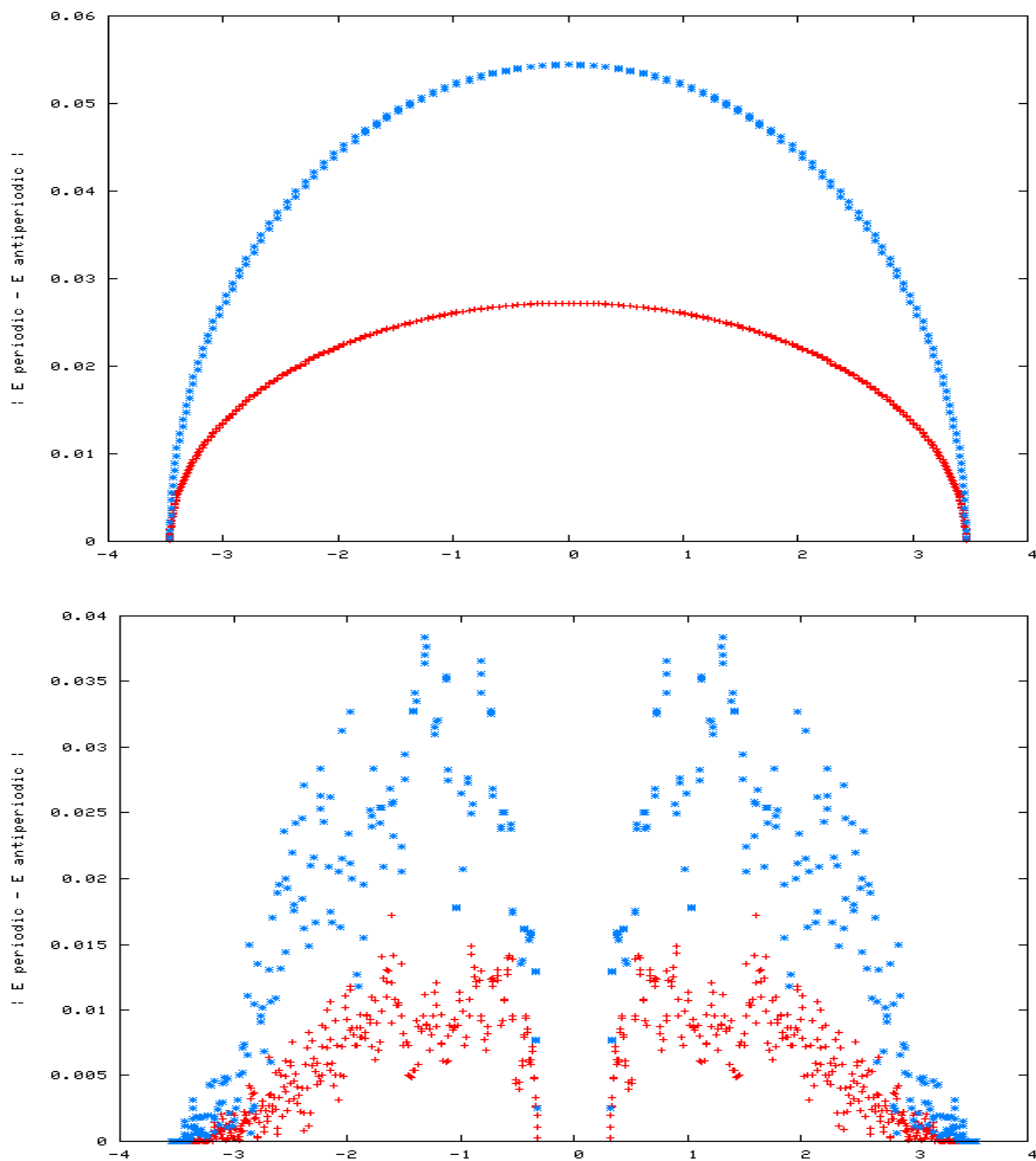
Consistency requires

$$E = \pm \sqrt{9 - 4 \sin^2 \arg \eta} = \pm \sqrt{6}$$

in which case *any* sequence $\{\alpha_z\}_{z \in \mathbf{Z}}$ provides an eigenfunction, with

$$\beta_z = \pm \frac{3 - 2 \sin \arg \eta}{\sqrt{6}} \alpha_{z-1}$$

Figure 5.1: Differences (vertical; absolute values) of energy eigenvalues (horizontal) obtained by numerical diagonalisation of (5.2) with periodic and antiperiodic boundary conditions for $z = 1 \dots 200$ (blue asterisks) and $z = 1 \dots 400$ (red crosses). In the upper graph, $k_x = k_y = \pi/2$; in the lower graph, $k_x = 1.5$, $k_y = 1.7$. For delocalised wavefunctions, differences should be of order mean level-spacing divided by the number of lattice sites [11]. Thus, wavefunctions at $k_x = k_y = \pi/2$ appear delocalised, while the lower figure suggests that, at energies close to zero, localisation occurs.



Chapter 6

Details of symmetry operations

6.1 Translational symmetries

Hamiltonian (2.1) with links (3.52) was derived under the assumption of plaquettes invariant under translations in the x and y direction. It must therefore, at least, have these invariances modulo gauge transformations. Since there is no y dependency in the expressions (3.52), strict invariance under unit translations in the y direction is an immediate symmetry of the Hamiltonian. In the x direction, translations $x \rightarrow x+1$ must be accompanied by a gauge transformation as defined in (2.5) with

$$g_X(y, z) = \lambda^{3y+3d(z)} \quad (6.1)$$

Assuming m to be the smallest number with

$$\lambda^{3m} = 1$$

the invariant subspaces under the group of the above x and y translations are spanned by linearly independent functions of the form

$$e^{i(xk_x+yk_y)} f(z), \lambda^{3y+3d(z)} e^{i(xk_x+yk_y)} f(z), \dots, \lambda^{(m-1)(3y+3d(z))} e^{i(xk_x+yk_y)} f(z)$$

where $f(z)$ is an arbitrary but fixed function. Hence, the multiplicities of energy levels will be multiples of m . For example, $\lambda = i$ leads to energetic quartets, octets, etc.

6.2 Wavefunctions rotated by 120 degrees

The Hamiltonian of a free fermion propagating on a lattice with 120° rotational symmetry was constructed from symmetric plaquettes in conjunction

with gauge fixing along specific directions. Clearly, the same energy eigenvalues are obtained (hence, degeneracy can be recovered) if the axes of the gauge fixing are rotated by 120° .

Another reason for considering details of 120° rotations is to obtain an indication of spin by composing three of such rotations. However, as is known from Susskind fermions on a simple cubic lattice, spin-half shows up by a global factor -1 only under 360° rotations about a centre such that *all* sites of the lattice are moved during the operation. This is because, if the rotation has a fixed point, *nothing* changes in a wavefunction concentrated at such a point. While for a cubic lattice any point of the dual lattice is an appropriate centre for making every site move under a rotation, we apparently have to compose 120° rotations by about three *different* centres on a random close-pack lattice.

6.2.1 About origin at $\mathbf{d}=0$

Choosing the centre at the origin $x = y = 0$ in the plane $z = 0$, the rotation of the polygon of gauge-fixing $\hat{4}$ and $\hat{7}$ links requires that at $z \neq 0$ the rotation about $x = y = 0$ be followed by a translation by $-d(z)\hat{1}$ (cf. definition (3.2)). Thus a function $f(x, y, z)$, when rotated counterclockwise by 120° , takes the form

$$f_{120}^{(0)}(x, y, z) = f(y - x - d(z), -x - d(z), z) \quad (6.2)$$

Applying the same rotation once more we obtain

$$f_{240}^{(0)}(x, y, z) = f_{120}^{(0)}(y - x - d, -x - d, z) = f(-y - d, x - y, z)$$

Since the link in direction $\hat{1}$ takes over the role of the original $\hat{3}$ etc., the 120° -rotation transforms (3.52) into

$$\begin{aligned} l'_1 &= \lambda^{3y-3x+3d(z)} \mu^3 \\ l'_2 &= 1 \\ l'_3 &= \lambda^{3x-3y+3d(z)} \\ l'_4 &= \lambda^{4d(z)+3} \mu^2 \zeta_z^{-1} \\ l'_5 &= \lambda^{3x-3y+3d(z)} \\ l'_6 &= \lambda^{3+3x-3y+5d(z)} \mu \zeta_z \\ l'_7 &= \lambda^{1-4d(z)} \mu^{-2} \zeta_z^{-1} \\ l'_8 &= \lambda^{3y-3x-3d(z)} \\ l'_9 &= \lambda^{2-3x+3y-5d(z)} \mu^{-1} \zeta_z \end{aligned}$$

This is equivalent to a gauge transformation $g(x, y, z)$, as defined in (2.5), of the links on the original lattice. Using $\zeta_z^3 = 1$ and equations (3.2) and (3.3) the gauge transformation is found to be

$$g_{120}^{(0)}(x, y, z) = \lambda^{3xy+3xd(z)-\frac{3}{2}x(x-1)+2d(z)^2+d(z)} \mu^{3x+2d(z)} r(z) \quad (6.3)$$

where

$$r(z+1) = r(z)\zeta_z^{-1}$$

The global phase is chosen such that, up to the Z_3 ambiguity in $r(z)$, there is no effect on a wavefunction concentrated at a fixed point $x = y = 0$, $d = 0$.

6.2.2 About origin at $d=0$ assuming (4.16)

If links take the form (4.16), the gauge factor of (6.3) simplifies to

$$g_{120}^{(0)}(x, y, z) = (-1)^{\frac{1}{2}x(x-1)+xy+(x+1)z} \eta^{3x+2z} \quad (6.4)$$

This can be written as a sum of plane-wave contributions, since for integer x and y

$$\begin{aligned} (-1)^{xy} &= \frac{1}{2} \left(1 + (-1)^x + (-1)^y - (-1)^{x+y} \right) \\ (-1)^{\frac{1}{2}x(x-1)} &= \frac{1-i}{2} i^x + \frac{1+i}{2} i^{-x} \end{aligned} \quad (6.5)$$

6.2.3 About origin at $d=1$

This case is different from the previous only because of the maximal gauge fixing (3.1) of the link variables. When only the motion of sites under the rotation is considered, the geometric situation is the same as with equation (6.2) except that the counting of d starts at the plane below the centre of rotation. Thus, replacing d by $d-1$ in (6.2) we obtain (where the superscript refers to the corresponding point in figure 3.1)

$$f_{120}^{(4)}(x, y, z) = f(y-x-d+1, -x-d+1, z) \quad (6.6)$$

x and y directions are rotated in the same way as in (6.2), but the fixed point now is at $x = 0$, $y = 0$ and $d = 1$. The links of (3.52) are transformed into

$$\begin{aligned} l'_1 &= \lambda^{3y-3x+3d+3} \mu^3 \\ l'_2 &= 1 \\ l'_3 &= \lambda^{3x-3y+3d-3} \\ l'_4 &= \lambda^{4d(z)+3} \mu^2 \zeta_z^{-1} \end{aligned}$$

$$\begin{aligned}
l'_5 &= \lambda^{3x-3y+3d-3} \\
l'_6 &= \lambda^{3x-3y+5d(z)} \mu \zeta_z \\
l'_7 &= \lambda^{1-4d(z)} \mu^{-2} \zeta_z^{-1} \\
l'_8 &= \lambda^{3-3x+3y-3d} \\
l'_9 &= \lambda^{5-3x+3y-5d} \mu^{-1} \zeta_z
\end{aligned}$$

These differ from the analogous links in section 6.2.1 by a factor $\lambda^{\pm 3}$ for links protruding by ± 1 in the x direction. Hence, the l' are equivalently obtained by the gauge transformation

$$g_{120}^{(4)}(x, y, z) = \lambda^{3xy+3xd-\frac{3}{2}x(x-1)+3x+2d^2+d-3} \mu^{3x+2d-2} r(z) \quad (6.7)$$

The global phase is chosen such that, up to the Z_3 ambiguity in the $r(z)$, there is no effect on a wavefunction concentrated at a fixed point $x = y = 0$, $d = 1$.

6.2.4 About shifted origin at $d=-1$

x and y directions are rotated in the same way as in the previous two sections, but the centre of rotation is at $x = 1$, $y = 0$ and $d = -1$ (point with number 8 in figure 3.1). Thus, considering only the motion of sites under the rotation,

$$f_{120}^{(8)}(x, y, z) = f(y - x - d + 1, -x - d, z) \quad (6.8)$$

This differs from (6.6) only by the transformation of the y coordinate, which does not occur in (3.52). Hence, the l' are the same as in section 6.2.3, and the corresponding gauge transformation coincides with (6.7) except for the global phase. For a wavefunction at the fixed point to remain unaffected (up to the Z_3 ambiguity) we must now choose

$$g_{120}^{(8)}(x, y, z) = \lambda^{3xy+3xd-\frac{3}{2}x(x-1)+3x+2d^2+d-1} \mu^{3x+2d-1} r(z) \quad (6.9)$$

6.3 Full-cycle rotation with no fixed point

Composing the rotations of (6.2), (6.6) and (6.8), the wavefunction returns to its original form, while the gauge transformations produce a global factor,

$$g_{120}^{(8)}(x, y, z) g_{120}^{(4)}(y - x - d + 1, -x - d, z) g_{120}^{(0)}(-y - d, x - y, z) = \lambda^{-1} \quad (6.10)$$

Because of the Z_3 ambiguity of the global phase in each of the three rotations, a Z_3 ambiguity persists in the global phase of the 360° rotation. In MAPLE

this is conveniently seen by using the following expressions for exponents and substitutions.

```

g0lambda := 3*x*y+3*x*d-3*x*(x-1)/2+2*d*d+d;
g4lambda := 3*x*y+3*x*d-3*x*(x-1)/2+2*d*d+d+3*x-3;
g8lambda := 3*x*y+3*x*d-3*x*(x-1)/2+2*d*d+d+3*x-1;
g0mu := 3*x+2*d; g4mu := 3*x+2*d-2; g8mu := 3*x+2*d-1;
S4:={x=y-x-d+1,y=-x-d+1}; S8:={x=y-x-d+1,y=-x-d};
simplify(g8lambda+subs(S8,g4lambda)+subs(S8,subs(S4,g0lambda)));
simplify(g8mu+subs(S8,g4mu)+subs(S8,subs(S4,g0mu)));

```

6.4 Rotational degeneracy

Let $\psi_E(x, y, z)$ be an eigenfunction of the Hamiltonian defined by (2.1), constructed under conditions (3.1). Then the rotated function

$$\psi'(x, y, z) = \psi_E(y - x - d, -x - d, z)$$

is an eigenfunction with the same energy for the 120° -rotated Hamiltonian, which consists of the rotated links. Since these are the original links gauge-transformed with (6.3), we may pull the gauge-transformation factors into the wave function ψ' , thus obtaining another (sometimes, the same) eigenfunction of the original Hamiltonian,

$$\psi_E^{(120)}(x, y, z) = g_{120}(x, y, z)\psi_E(y - x - d, -x - d, z) \quad (6.11)$$

Applying the same procedure once more we obtain

$$\psi_E^{(240)}(x, y, z) = g_{120}(x, y, z)g_{120}(y - x - d, -x - d, z)\psi_E(-y - d, x - y, z) \quad (6.12)$$

After a third rotation we recover the original eigenfunction.

6.5 Periodic boundary conditions

Symmetries under planar translations and 120° rotations are preserved by planar periodic boundary conditions

$$\begin{aligned} \psi(x + N, y, z) &= \psi(x, y, z) \\ \psi(x, y + N, z) &= \psi(x, y, z) \end{aligned} \quad (6.13)$$

Periods in the $\hat{1}$ and $\hat{2}$ direction are equal as required by the 120° rotational symmetry. Periodicity in the $\hat{3}$ direction, $\psi(x - N, y - N, z) = \psi(x, y, z)$,

is automatically satisfied in this case. In a numerical representation, the planar sites are addressed the same way as on a cubic lattice. That is, a non-redundant set of sites has x and y coordinates running independently from 1 to N .

Quasi-periodic boundary conditions in the perpendicular z direction,

$$\psi(x, y, z + M) = e^{i\alpha} \psi(x, y, z) \quad (6.14)$$

may be useful for defining the component of momentum in this direction (for which there is no lattice translational symmetry). The length of the period in the z direction must be consistent with the sequence of $\hat{4}$ and $\hat{7}$ directions. In order to be able to identify the plane of $z = M$ with the plane at $z = 0$, the xy components of the interplanar shifts must sum up to zero, so the number of $\hat{4}$ and $\hat{7}$ shifts within the period must be equal. In terms of the displacement function (3.2),

$$d(z + M) = d(z)$$

Bibliography

- [1] L. Susskind, Phys. Rev. D **16** (1977) 3031.
- [2] M. Creutz, *Quarks, gluons and lattices* (Univ. Pr., Cambridge, 1983).
- [3] A. Zee, in *M. A. B. Bég Memorial Volume*, edited by A. Ali and P. Hoodbhoy (World Scientific, Singapore, 1991), pp. 129–140 .
- [4] L. Polley, arXiv:quant-ph/0110175v1.
- [5] N. W. Ashcroft and N. D. Mermin, *Solid state physics* (Saunders College Publ., Fort Worth, 1995), international ed., 21. print.
- [6] T. Aste and D. Weaire, *The pursuit of perfect packing* (Institute of Physics Publishing, London, 2000).
- [7] R. Jackiw and S.-Y. Pi, Phys. Rev. Lett. **98** (2007) 266402.
- [8] P. Maraner and J. K. Pachos, Phys. Lett. A **373** (2009) 2542, arXiv:0807.0826v2.
- [9] A. Duncan, Phys. Rev. D **37** (1988) 563.
- [10] B. Kramer and A. MacKinnon, Rep. Prog. Phys. **56** (1993) 1469.
- [11] J. T. Edwards and D. J. Thouless, J. Phys. C: Solid State Phys. **5** (1972) 807.